International Journal of Nanomedicine

Dovepress

open access to scientific and medical research

Open Access Full Text Article

ORIGINAL RESEARCH

Directional Osteo-Differentiation Effect of hADSCs on Nanotopographical Self-Assembled Polystyrene Nanopit Surfaces

This article was published in the following Dove Press journal:
International Journal of Nanomedicine

Changhong Zhao[1]
Xuebin Song[1]
Xiaoyuan Lu[2]

[1]School of Life Sciences and Technology, Xinxiang Medical University, Xinxiang, Henan, 453003, People's Republic of China; [2]College of Medical Engineering, Xinxiang Medical University, Henan 453003, People's Republic of China

Introduction: Cells exhibit high sensitivity and a diverse response to the nanotopography of the extracellular matrix, thereby endowing materials with instructive performances formerly reserved for growth factors. This finding leads to opportunities for improvement. However, the interplay between the topographical surface and cell behaviors remains incompletely understood.

Methods: In the present study, we showed nanosurfaces with various dimensions of nanopits (200–750 nm) fabricated by self-assembling polystyrene (PS) nanospheres. Human adipose-derived stem cell behaviors, such as cell morphology, adhesion, cytoskeleton contractility, proliferation, and differentiation, were investigated on the prepared PS nanopit surface.

Results: The osteogenic differentiation can be enhanced by nanopits with a diameter of 300–400 nm.

Discussion: The present study provided exciting new avenues to investigate cellular responses to well-defined nanoscale topographic features, which could further guide bone tissue engineering and stem cell clinical research. The capability to control developing biomaterials mimicking nanotopographic surfaces promoted functional tissue engineering, such as artificial joint replacement, bone repair, and dental applications.

Keywords: osteo-differentiation, nanotopography, polystyrene

Introduction

Current studies that focus on cell response to the surrounding nanotopography provide us with new directions in the field of tissue engineering and regenerative medicine.[1] The nanotopography of a material surface plays an important role on the regulation of mesenchymal stem cell (MSC) differentiation with comparable efficiency to chemical treatments.[2–4] Given the hierarchically composed structure of bone, osteogenic cells are surrounded by various topographical features with different sizes in a mineralized organic matrix environment, as follows: macrofeatures such as cell morphology, collagen fiber networks, calcium phosphate mineral crystallites, and interconnecting honeycomb pores.[5,6] Cells can "sense" substrate topography, morphology, elasticity, and surface patterns ranging from 10 nm to 100 μm,[7] by the cellular sensory machinery which can integrate such complex nanoscale physical information at the cell/extracellular matrix (ECM) interface into a biochemical environmental signal to regulate intracellular signaling and the corresponding cell function.[8,9] The surface roughness at the micro/

Correspondence: Changhong Zhao
Tel/Fax +86 373 3029444
Email 15921061530@163.com

submit your manuscript | www.dovepress.com
DovePress
http://doi.org/10.2147/IJN.S240300

nanoscale promotes osseointegration by enhancing cell differentiation and local factor production.[10–12] Therefore, designing implant surfaces with unique topographical structures has become necessary. They have great potential for the manufacturing of future superior orthopedic implants.

Recently, the nanoscale surface topography was proven to have highly promising effects on regulating survival, proliferation, migration, and differentiation of adult MSCs.[13,14] Implant materials with nanostructured surfaces have shown promising applications in orthopedic surgical field.[15] The nanoscale surface morphology remarkably determines cellular responses, which have an important role in the optimization of medical implant biocompatibility.[16] However, the exact mechanism underlying a cell's response to these fundamental nanoscale surface topographic features remains unclear. The existing knowledge does not prescribe the optimal nanotopography for a specific biomedical application and the possible surface patterns that could be the optimal nanotopography for a specific biomedical application.[17] Therefore, to obtain desirable cellular responses, well-defined nanoscale topographic features with tunable parameters are required for a particularly designed implant surface.[18] The development of precisely controllable nanoscale surface topographic features for cell response study is necessary and important, thereby leading to the comprehensive understanding of the determination of cellular behavior and cell fate through topographic features.

However, most of the existing works on nanotopography for cell study relies on complex and expensive nanofabrication processes, such as nanoimprint lithography and electron beam to make nanoscale surface structures for investigating cellular responses. In the present study, polystyrene (PS) nanospheres with different diameters (200–750 nm) were prepared on glass substrates by a simple one-step self-assembly method. Human adipose-derived stem cells (hADSCs), as one of the autologous stem cells for tissue regeneration, were evaluated for their behavior after being in contact with varied sizes of PS nanopits. With varying diameter of nano-PS spheres (from 200 nm to 750 nm, defined as PS-200 to PS-750), well-ordered and periodically arranged nanostructures were obtained, and the effect of nanostructures on hADSCs osteogenic differentiation was systemically studied.

Materials and Methods

Preparation of PS Nanopit Surfaces

Monodispersed PS spheres with uniform size distribution and variable sizes (diameter from 200 nm to 750 nm) were purchased from Alfa Aesar Chemical Co., Ltd., Shanghai, China. The round SiO_2 substrates (diameter 13.5 mm, thickness 1 mm) were ultrasonically cleaned with water (5 min), acetone (10 min), and alcohol (10 min). Then, they were rinsed with deionized water and dried with nitrogen. A piranha solution was used to make the substrates highly hydrophilic and easily bond with PS spheres by immersing SiO_2 in the solution at 80°C for 1 h. A monolayer hexagonal close-packed array of monodispersed PS spheres with diameters from 200 to 750 nm were formed on a SiO_2 surface using a self-assembly process[19] by vertically inserting the clean substrates into various PS solution with different PS sphere sizes.

Surface Characterization

The morphology of PS nanopit surfaces was observed by scanning electron microscopy (SEM), and the diameters of the PS spheres were measured using image J software (https://imagej.nih.gov/ij/; National Institute of Health, Bethesda, MD, USA).

Cell Culture

hADSCs were purchased from Cyagen Biosciences, China. hADSCs were cultured with basal α-MEM medium supplemented with 10% fetal bovine serum and 1% penicillin-streptomycin and incubated at 37°C and 5% CO_2.

Cell Morphology, Attachment, Viability, and Proliferation

Cell morphology, spreading, viability, and proliferation on PS nanopit surfaces, SiO_2 flat control, and tissue culture plates (TCP) were investigated. The samples were placed into 24-well plates for sterilization by immersing into 75% ethanol overnight and washing with sterile phosphate-buffered saline (PBS) prior to use. A total of 20,000 cells per well were seeded on the samples and control surfaces. For cell morphology and adhesion observation, hADSCs were stained by fluorescein diacetate (FDA) and propidium iodide (PI) after culturing for 24 h and then observed by confocal laser scanning microscopy (CLSM).

Cell morphology and spreading on the samples were also detected with SEM. After culturing for 24 h, cells were fixed with 2.5% glutaraldehyde, dehydrated with

gradient ethanol solution. Then, they were subjected to supercritical point drying. Cells were sputter-coated with gold prior to observation by SEM.

Cell proliferation on PS nanopit surfaces was determined by cell counting kit-8 (CCK-8). After culturing for 1, 4, and 7 days, the absorbance of the culture medium after incubation with CCK-8 was assayed by a microplate reader at 450 nm. FDA/PI staining was also performed at 1, 4, and 7 days to directly visualize living and dead cells to determine hADSC viability.

Alkaline Phosphatase (ALP) Activity Assay

After culturing for 1, 7, 14, and 21 days, the hADSCs on different substrates were digested from the samples and transferred into centrifuge tubes, washed with PBS, and centrifuged. The remaining cell pellet was resuspended in 0.2% Nonidet P-40 solution and sonicated in ice-water bath for 2 min. The ALP activity at different time points was analyzed using a fluorescence-based ALP detection kit.

Quantitative Polymerase Chain Reaction (PCR)

The cellular RNA was extracted from hADSCs after culturing on PS nanopit surfaces for 7, 14, and 21 days. Next, the concentration and purity of RNA were determined by a Q-5000 spectrophotometer at 260/280 nm[7]. The expression of Col1, Runx2, OCN, OPN, and β-actin utilized for the normalization of any differences in the amount of total RNA was quantified by a 7500 Real-Time PCR system. The relative transcript levels of the target gene were normalized to β-actin and expressed as the mean ± SD (n = 3 for each group).

Cell Immunohistochemical Staining Analysis for Osteogenesis Differentiation

The hADSCs were seeded on PS nanopits and control surfaces and cultured for 21 days for cell immunohistochemical staining analysis. Briefly, cells were fixed with 4% paraformaldehyde solution for 10 min and then permeabilized with 0.2% Triton X-100 for 10 min. The fixed cells were blocked with 10% goat serum for 30 min at 37°C and then incubated with primary antibodies against osteocalcin (mouse monoclonal anti-OCN) and osteopontin (rabbit polyclonal anti-OPN) at 4°C for 12 h. For OPN and OCN staining, cells were incubated with Alexa Fluor 488-labeled secondary antibodies (goat anti-rabbit and goat anti-mouse, respectively) in 5% goat serum for 30 min at 37°C. After staining, the cells were washed with PBS and stained using phalloidin-conjugated Alexa Fluor 568 (30 min, for F-actin) and Hochest 33,258 (10 min, for nuclei). Finally, CLSM was used for immunohistochemical analysis.

The ALP activity and calcium deposition of hADSCs on the samples were also stained using ALP staining kit and alizarin red staining kit, respectively, according to the manufacturer's instruction. The results were observed and photographed by an optical microscope with a digital camera.

Statistical Analysis

The data between groups were analyzed using one-way ANOVA in GraphPad Instant software. Data were reported as mean ± standard deviation; $P < 0.05$ or 0.01 was considered significant (n = 3).

Results

PS Nanopit Surface Morphology

The PS nanopits with various diameters were prepared and characterized by SEM (Figure 1). The PS nanospheres with average diameters of 200, 300, 400, 500, 600, and 750 nm were self-assembled onto SiO_2 substrates. The pure SiO_2 substrate control was characterized as 0 nm. Moreover, flat TCP surfaces were characterized as blank control. A bottom-up self-assembling strategy was utilized to form an arrayed architecture of nanopits. SEM demonstrated that well-defined diameter and mono-dispersed PS nanospheres were formed on the flat SiO_2 surfaces.

Cell Morphology of hADSCs

The morphology of cells was visualized by using SEM (Figure 2). Cultured cells grew alone the nanopits and showed distinguished morphology. On TCP, flat SiO2 surface (0 nm) and PS-200, PS-300, PS-400, cells showed a random morphology. However, cells exhibited an elongated morphology on PS-500, PS-600, PS-750. Cells on PS-500 to 750 exhibited poor spreading, whereas those on PS-300, PS-400 had much larger spreading area, which means that PS-300, PS-400 strengthened cell adhesion and spreading.

Cell Viability and Proliferation of hADSCs

The viability and proliferation of hADSCs on PS nanopits were investigated using live/dead staining and cck-8 assay.

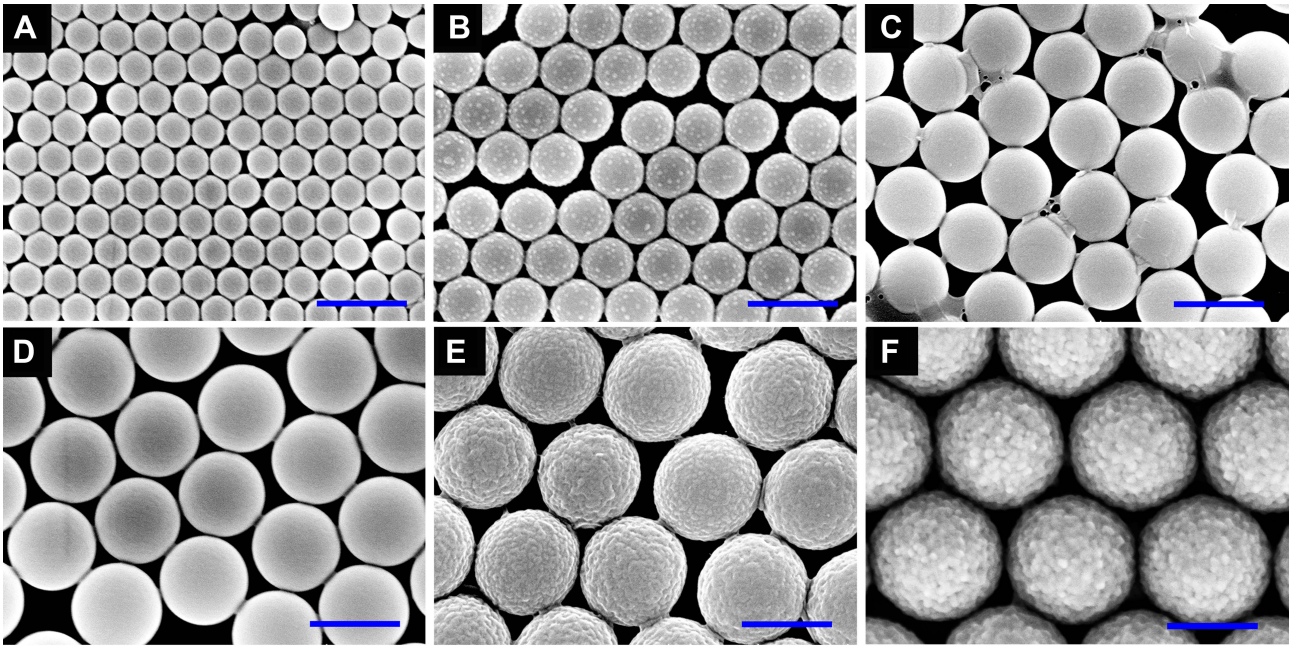

Figure 1 SEM images of PS nanopits with various diameters on SiO2 substrates: (**A**) 200 nm, (**B**) 300 nm, (**C**) 400 nm, (**D**) 500 nm, (**E**) 600 nm, and (**F**) 750 nm (scale bar = 500 nm).

As shown in Figure 3, almost no dead cells were found on the flat TCP to PS-400. The number of dead cells slightly increased within PS-600 to PS-750 at day 7, but all topographies showed good cytocompatibility, and only less than 10% of dead cells were found on PS-750, thereby indicating good cytocompatibility after the construction of PS nanopit-topography. Figure 3B shows that cells on PS-750 had lower viability values than that on the flat TCP to PS-600 at day 1 ($P < 0.01$). At days 4 and 7, PS-600 and PS-750 showed poorer viability than the flat TCP to PS-500 ($P < 0.05$). Cell proliferation results showed that hADSCs proliferated on all substrates with time increasing from day 1 to day 7. PS-300 and PS-400 considerably promoted cell proliferation compared with PS-600 and

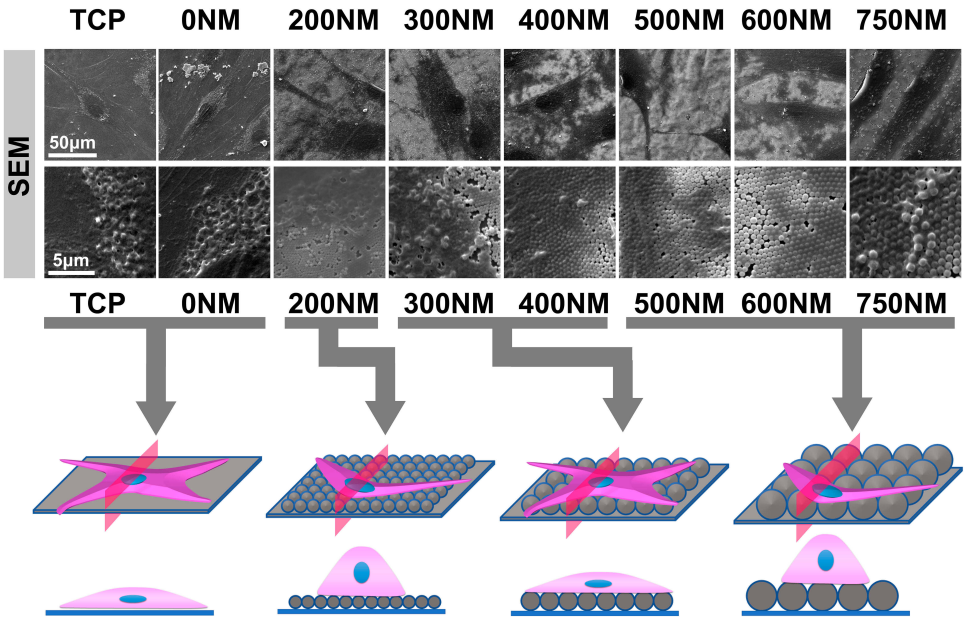

Figure 2 SEM images and cell morphology model of hADSCs on TCP and nanopits after 1 day of culturing.

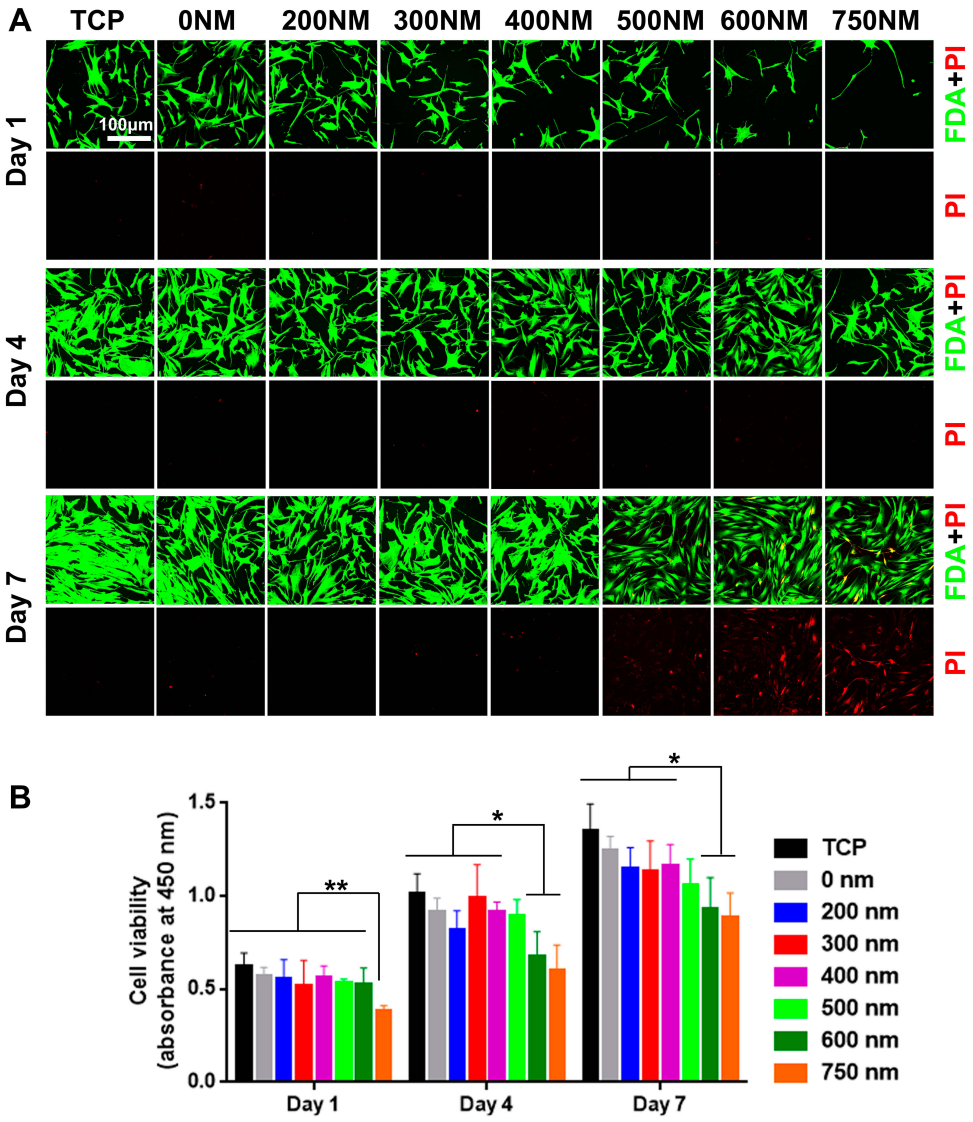

Figure 3 (**A**) Viability and (**B**) proliferation of hADSCs on TCP and various PS nanopits for 1, 4, and 7 days. *P < 0.05; **P < 0.01.

PS-750. These results are consistent with the observation presented in Figure 2, as the cells showing better spread on PS-300 and PS-400 than the others.

Cell Differentiation of hADSCs

Three principal periods were identified in the whole osteogenic differentiation process: cell proliferation, ECM maturation, and matrix mineralization. ALP activity is one of the earliest phenotypic markers for osteogenic differentiation.[20] ECM is a complex and heterogeneous network of adhesive protein and growth factors that support and guide cells. Cell immunohistochemical staining analysis results are shown in Figure 4A. Cells on PS-500 to 750 showed elongated and thin morphology, which was similar to CLSM and SEM images in Figure 2. Compared with flat TCP and PS-200 to PS-400, the spreading area of cells was generally smaller on PS-500, PS-600, and PS-750, and cell spread seemed limited. The reason could be the different distances and spaces between the neighboring pits with different diameters of PS nanospheres. For example, the diameter of the PS nanospheres on PS-500 was approximately 500 nm, and the space and distance between the nanopits can be close to 500 nm. Thus, crossing the distance from one pit to another might be difficult for cells. The suitable distance and space for hADSC spread on PS nanopits could be between 0 and 400 nm. Moreover, the distinct morphology of hADSCs could be caused by different diameters of pits which caused different stretching resistance, thereby affecting the rearrangement of cytoskeleton. As shown in Figure 4, the cell

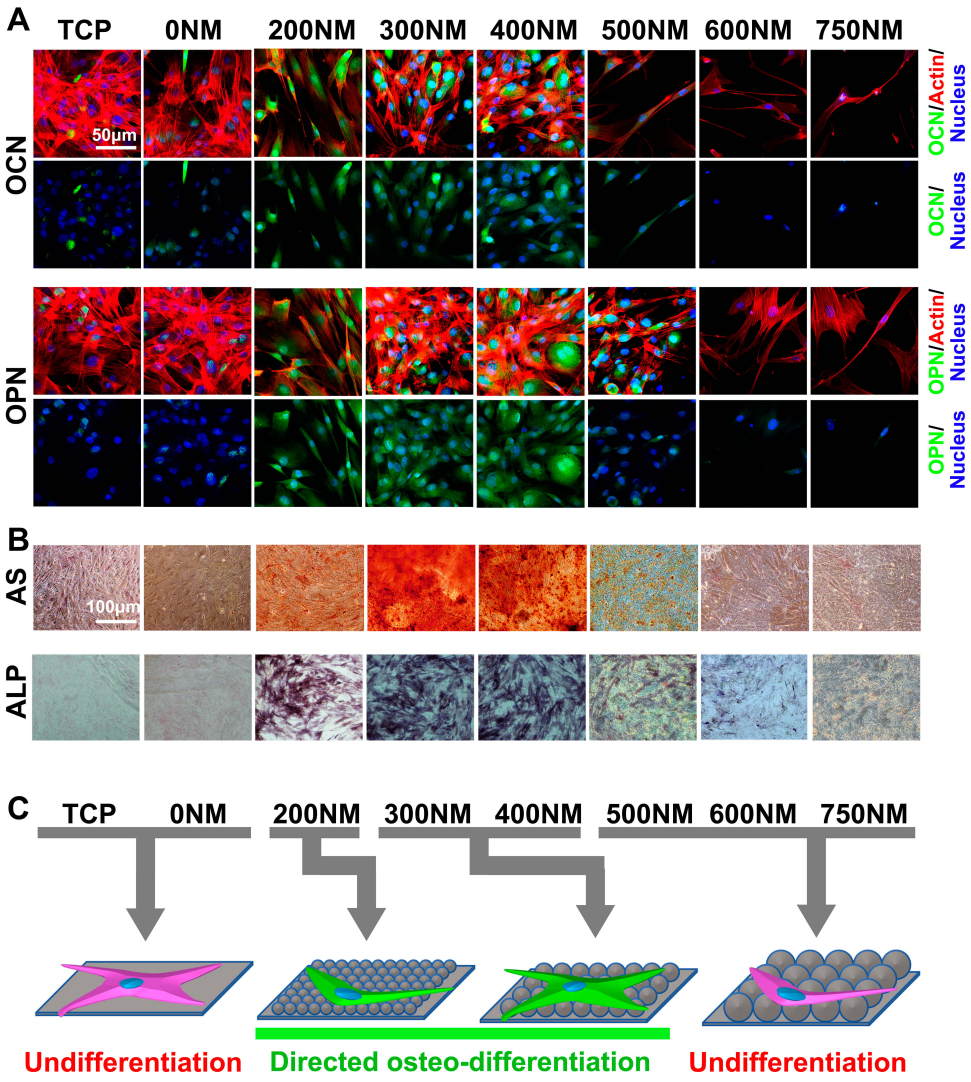

Figure 4 Directional differentiation of hADSCs on TCP and PS nanopits. (**A**) Immunohistochemical staining of OCN and OPN in ADSCs grown on TCP and PS nanopits on day 21. The bars are 30 μm. (**B**) Alizarin red S (ARS) staining of calcium deposition (Ca) of ADSCs grown on TCP and PS nanopits on day 21. The bars are 100 μm. (**C**) Schematic of directional differentiation of hADSCs on TCP and PS nanopits.

cytoskeleton dramatically changed with increasing nanopit diameter up to 500 nm. Consistently, for actin staining, the fluorescent intensities on PS-300 and PS-400 were higher than those on PS-200, PS-500, PS-600, and PS-750. Vinculin is an important protein that affects stem cell differentiation to a large extent, and high expression of vinculin may result in high degree of osteogenic differentiation.[21] This finding could explain the osteogenic differentiation of hADSCs improved by PS-300 and PS-400.

To investigate the effect of PS nanopits on the osteogenic differentiation of hADSCs, ALP expression was analyzed (Figures 4B and 5A). The ALP-stained images (Figure 4B) 21 days after culture showed the highest color intensity for PS-300, thereby indicating the highest ALP expression. ARS staining of calcium deposition (Figure 4B) showed the same trend. The highest level of calcium deposition was found on PS-300. Quantitative analysis of ALP activity (Figure 5A) showed that at all time points (days 1, 4, 7, 14, and 21), PS-200, PS-300 and PS-400 had the top three highest levels of ALP activity, whereas PS-600 and PS-750 had the lowest levels. PS-300 showed maximum ALP expression compared with TCP and other surfaces at day 14, which was consistent with the ALP staining results.

In addition, other osteogenic differentiation-related gene markers (COL1, OCN, OPN, and RUNX2) were also upregulated for PS-200 to 400 (Figure 5B) at all time points (day 7, 14, and 21). PS-300 showed the highest level of gene expression for all gene makers at all time points.

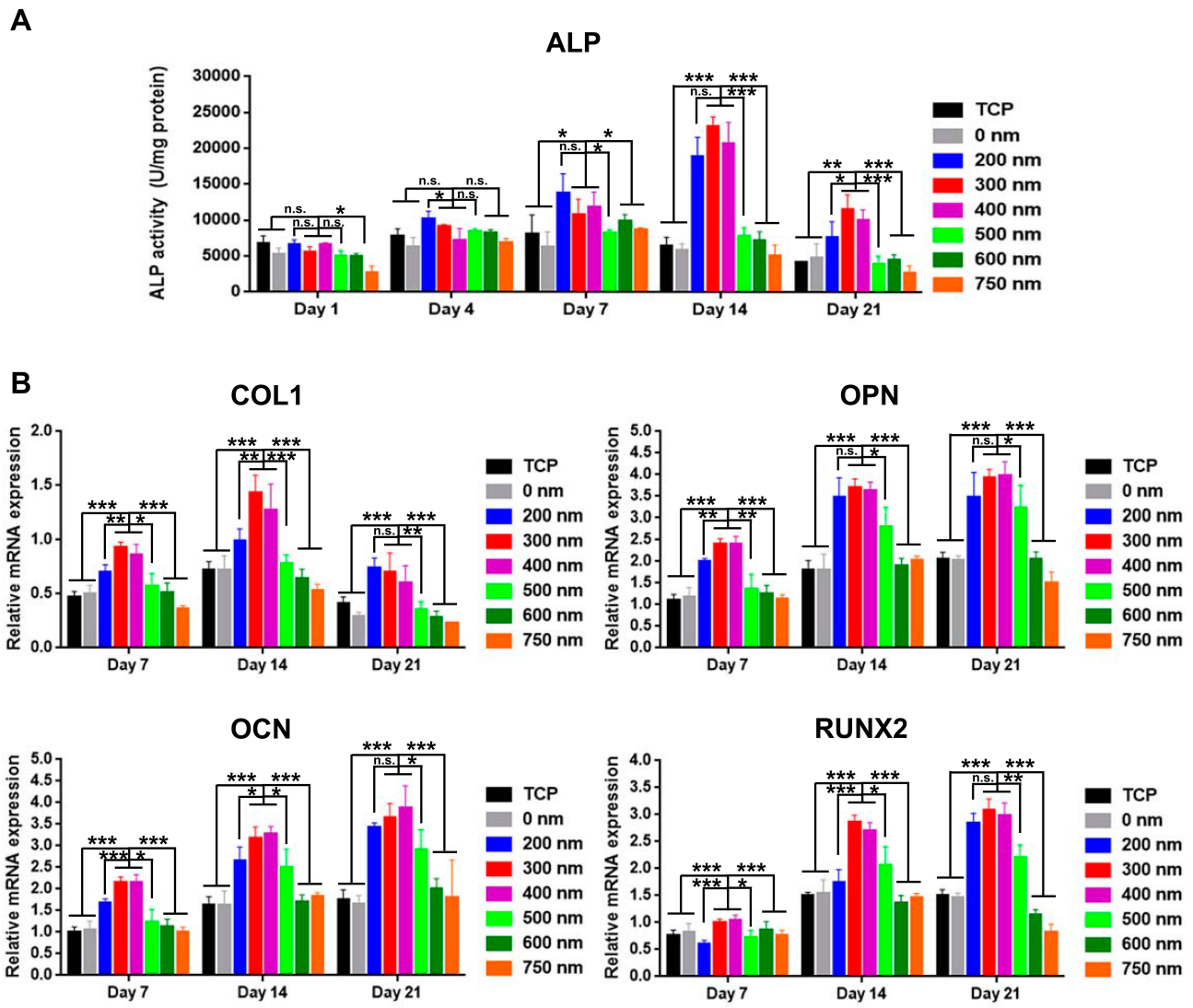

Figure 5 ALP and gene marker expression levels of hADSCs on TCP and PS nanopits for 1, 7, 14, and 21 days. (**A**) ALP expression concentration of hADSCs on TCP and PS nanopits. (**B**) Quantitative real-time polymerase chain reaction (qRT-PCR) of gene marker expression of hADSCs on TCP and PS nanopits for 7, 14, and 21 days. The y-axis represents the relative expression (2-ΔCT) normalized to the expression level of the housekeeping gene GAPDH. COL1: collagen type-1; OPN: osteopontin; OCN: osteocalcin; Runx2: runt-related transcription factor 2. *P < 0.05; **P < 0.01; ***P < 0.005.

Combining all the results, we can conclude that osteogenic differentiation was remarkably enhanced by PS-200 to PS-400, particularly by PS-300.

Discussion

Despite much efforts to develop an optimal topographical surface to enhance osteogenic differentiation, studies have been conducted with limited cell types and patterns.[22] Several nanoscale topographical features, such as pillars,[23–25] grooves,[10,26] grids,[27] or other pattern features[24,28,29] but rarely nanopits, are used for studying differentiation of hADSCs. To advance in this field, various strategies have been tested to fabricate nano-sized surfaces. Traditional methods include photolithography or electron beam. However, these methods share the same disadvantages, such as high cost, long fabrication process (polishing substrate, spinning coating, exposure, and etching process), and clean room requirement. For nanotopography fabrication, electronic beam lithography exposure process is generally time-consuming. On the contrary, direct laser printing is not limited by laser diffraction, which mostly generates period patterns on a micrometer scale. Interestingly, the self-assembly method shows great potential in fabricating nanoscale patterns in a simple and fast way.[30] Nanoscale surface topographical cues can be tailored to regulate stem cell fate in a similar way as the

ECM.[31] Understanding the cell–material interaction particularly on a well-defined surface is important for fundamental stem cell research and biomedical applications of implants, particularly on nano-sized surfaces. Thus, the present study has proven that nanostructured topography with different sizes of PS nanospheres can regulate the cell function of hADSCs in the absence of any exogenous factors.

The actin-cytoskeleton and cytoskeletal tension play important roles for stem cell behavior by regulating cell anchorage.[32] In the present study, a remarkable difference in actin-extensions of hADSCs was observed on various PS nanopit surfaces. The hADSCs showed enhanced cell attachment and actin extensions on PS-300 and PS-400 compared with the other PS nanopits (200, 500, 600, and 750 nm), indicating that 300–400 nm nanopit topography provided better space and distance for the formation of actin-cytoskeleton, cell anchorage, and spread.

The unique nanotopography has also been proven to trigger different cellular responses, such as cell adhesion, proliferation, and differentiation.[33] Cellular responses to a biomaterial surface are closely related to the surface chemistry and surface topographical structures.[34] In the present study, the effects of surface chemistry can be ignored, because the same PS material is used for fabricating the surface. The only difference was the diameter of the PS nanosphere. Evident differences were found for cells on the PS-500 to PS-750. Cells showed a more distinguished morphology than that on other nanopits. Cells respond to topographical features by changing their morphology, focal adhesion, and cytoskeleton. At the smooth surface and small size of nanopit surface, cells exhibited a good spreading behavior. However, cell spreading was less when the size increased (500–750 nm). In this case, the skeleton of cell changed with increasing topographic parameter. The observed effects of nanopits on cell behavior may be attributed to integrin-mediated cell adhesion regulation. Focal contact formation was impaired when the neighboring pit distance was larger than 400 nm. In addition, the viability of hADSCs showed a remarkable decrease when the nanopit diameter was larger than 400 nm. Similar effects of nano-topography on cell morphology were observed (Figure 3). The results of the present study are consistent with those of previous studies, in which the ability of nanotopography could modulate cell adhesion and spread. Our study provided the precise parameter (300–400 nm) of PS nanopits that can improve hADSC adhesion and spread.

A previous study suggested that nanogroove patterns enhance osteogenesis, because these patterns provide suitable mechanical stimulation, which is generally considered to be a key factor for osteogenesis.[35] An upregulation of focal adhesion kinase (an osteogenesis promoter) is found when osteoblasts are cultured on specific microgroove patterns. Reports speculating the possible signaling proteins involved in the mechanotransduction are identified.[36] A signaling pathway may be involved and triggered by specific nanoscale topographical cues for regulating hADSC osteogenic differentiation when cells are in contact with corresponding biochemical stimuli. These works demonstrated that surface topographical features can trigger a related signaling pathway that elicits specific cell response when synergizing with corresponding biochemical stimuli.[35] However, nanotopography alone without biochemical stimuli cannot govern cellular differentiation. By contrast, our study evidently showed that PS nanopits (300 and 400 nm) remarkably enhanced hADSC osteogenic differentiation in the absence of growth factors and other biochemical stimuli.

The upregulated differentiation on PS-300 and PS-400 surfaces may be due to different reasons. First, the enhanced cell adhesion, including more integrin clusters and vinculins on samples, triggers faster cell proliferation to reach confluence and subsequently stimulates higher differentiation.[37] Second, the hADSC spreading was improved by PS-300 and PS-400. The nuclear expansion may be induced by the spreading of cell filaments through mechanotransduction.[38] Such nuclear expansion can lead to the upregulated gene expression of bone-specific gene markers, such as ALP, OCN, and OPN, which was confirmed by quantitative PCR (Figure 5). Notably, PS-300 and PS-400 showed enhanced hADSC osteogenic differentiation compared with TCP and SiO_2 surfaces, without improving cell proliferation of hADSCs compared with the controls (Figure 3). Therefore, the enhanced osteogenic differentiation by PS-300 and PS-400 could mostly be attributed to the upregulated gene expression of OCN and OPN coursed by higher cell spreading of cell filaments (Figure 2).

Recently, Liu's group[39] developed polylactic acid (PLA) nanopillar arrays using anodic aluminum oxide nanowell arrays as templates. The prepared PLA nanopillar arrays have the same center-to-center distance but different diameters (100, 200, and 300 nm). Their study indicated that hADSC differentiation can be driven by nanopillar arrays, particularly by nanopillar arrays with a diameter of 200 nm. Another study suggested that nanopillar arrays (silicon

nanopillar arrays with critical dimensions in the range of 40–200 nm) can enhance osteogenic differentiation of human mesenchymal stem cells.[14] Although different nanostructure surfaces are used, the specific cell responses to nanoscale topography are confirmed in the present study. Moreover, the present study offers a new nanopit structure with directional osteo-differentiation effect of hADSCs.

Conclusion

We reported a facile yet effective self-assembling strategy for precise control and patterning of PS nanotopography. We demonstrated that hADSCs were intrinsically sensitive to the nanoscale topological cue and responded to PS nanopit surfaces. Some of the responses were as follows: reducing cell spreading, enhancing cell adhesion, and enhancing osteogenic differentiation. We provided direct experimental evidence showing that the osteogenic proliferation can be enhanced by nanopits with a diameter of 300–400 nm. The current work provided in-depth knowledge on topographical features that influence or control stem cell osteogenic differentiation and developed a nanoscale model surface that could be used as a platform for further stem cell–nanotopography interaction study.

Acknowledgments

The current work was supported by the National Science Foundation, China (Contract no. 51272153), the Key Scientific Research Projects of Higher Education of Henan Province (18A430026), and the Research Project of Henan Provincial Department of Science and Technology (Grant No.182102210122). The authors would like to thank Dr Mingyu Zhu, Department of Materials Science and Engineering, Southern University of Science and Technology, for revising and proofreading the manuscript.

Disclosure

The authors declare that they have no conflict of interest.

References

1. Hussey GS, Dziki JL, Badylak SF. Extracellular matrix-based materials for regenerative medicine. *Nat Rev Mater*. 2018;3:159–173.
2. Dalby MJ, Gadegaard N, Tare R, et al. The control of human mesenchymal cell differentiation using nanoscale symmetry and disorder. *Nat Mater*. 2007;6(12):997. doi:10.1038/nmat2013
3. Kang KB, Lawrence BD, Gao XR, Guaiquil VH, Liu A, Rosenblatt MI. The Effect of Micro- and Nanoscale Surface Topographies on Silk on Human Corneal Limbal Epithelial Cell Differentiation. *Sci Rep*. 2019;9(1):1507. doi:10.1038/s41598-018-37804-z
4. Lou H-Y, Zhao W, Zeng Y, Cui B. The role of membrane curvature in nanoscale topography-induced intracellular signaling. *Acc Chem Res*. 2018;51(5):1046–1053. doi:10.1021/acs.accounts.7b00594
5. Stevens MM, George JH. Exploring and engineering the cell surface interface. *Science*. 2005;310(5751):1135. doi:10.1126/science.1106587
6. Flemming RG, Murphy CJ, Abrams GA, Goodman SL, Nealey PF. Effects of synthetic micro- and nano-structured surfaces on cell behavior. *Biomaterials*. 1999;20(6):573–588. doi:10.1016/S0142-9612(98)00209-9
7. Dunn GA, Heath JP. A new hypothesis of contact guidance in tissue cells. *Exp Cell Res*. 1976;101(1):1–14. doi:10.1016/0014-4827(76)90405-5
8. Rangamani P, Lipshtat A, Azeloglu Evren U, et al. Decoding information in cell shape. *Cell*. 2013;154(6):1356–1369. doi:10.1016/j.cell.2013.08.026
9. Lou H-Y, Zhao W, Li X, et al. Membrane curvature underlies actin reorganization in response to nanoscale surface topography. *Proc National Acad Sci*. 2019;116:23143–23151.
10. Kim C-S, Kim J-H, Kim B, et al. A specific groove pattern can effectively induce osteoblast differentiation. *Adv Funct Mater*. 2017;27(44):1703569. doi:10.1002/adfm.201703569
11. Luu TU, Gott SC, Woo BWK, Rao MP, Liu WF. Micro- and nano-patterned topographical cues for regulating macrophage cell shape and phenotype. *ACS Appl Mater Interfaces*. 2015;7(51):28665–28672. doi:10.1021/acsami.5b10589
12. Fukuda N, Kanazawa M, Tsuru K, et al. Synergistic effect of surface phosphorylation and micro-roughness on enhanced osseointegration ability of poly(ether ether ketone) in the rabbit tibia. *Sci Rep*. 2018;8(1):16887. doi:10.1038/s41598-018-35313-7
13. Yim EKF, Leong KW. Significance of synthetic nanostructures in dictating cellular response. *Nanomedicine*. 2005;1(1):10–21. doi:10.1016/j.nano.2004.11.008
14. Pedrosa CR, Arl D, Grysan P, et al. Controlled nanoscale topographies for osteogenic differentiation of mesenchymal stem cells. *ACS Appl Mater Interfaces*. 2019;11(9):8858–8866. doi:10.1021/acsami.8b21393
15. Nair LS, Laurencin CT. Nanofibers and nanoparticles for orthopaedic surgery applications. *J Bone Joint Surg Ser A*. 2008;90(Suppl 1):128–131. doi:10.2106/JBJS.G.01520
16. Tran N, Webster TJ. Nanotechnology for bone materials. *Wiley Interdiscip Rev Nanomed Nanobiotechnol*. 2009;1(3):336–351. doi:10.1002/wnan.23
17. Unadkat HV, Hulsman M, Cornelissen K, et al. An algorithm-based topographical biomaterials library to instruct cell fate. *Proc National Acad Sci*. 2012;109:5905.
18. Motemani Y, Greulich C, Khare C, et al. Adherence of human mesenchymal stem cells on Ti and TiO2 nano-columnar surfaces fabricated by glancing angle sputter deposition. *Appl Surf Sci*. 2014;292:626–631. doi:10.1016/j.apsusc.2013.12.022
19. Jiang W-S, Xin W, Chen S-N, et al. Microshell arrays enhanced sensitivity in detection of specific antibody for reduced graphene oxide optical sensor. *Sensors (Basel)*. 2017;17(2):221. doi:10.3390/s17020221
20. Lian JB, Stein GS. Development of the osteoblast phenotype: molecular mechanisms mediating osteoblast growth and differentiation. *Iowa Orthop J*. 1995;15:118–140.
21. Holle AW, Tang X, Vijayraghavan D, et al. In situ mechanotransduction via vinculin regulates stem cell differentiation. *Stem Cells*. 2013;31(11):2467–2477. doi:10.1002/stem.1490
22. Huang J, Chen Y, Tang C, et al. The relationship between substrate topography and stem cell differentiation in the musculoskeletal system. *Cell mol life sci*. 2019;76:505–521.
23. Ahn EH, Kim Y, Kshitiz ASS, et al. Spatial control of adult stem cell fate using nanotopographic cues. *Biomaterials*. 2014;35(8):2401–2410. doi:10.1016/j.biomaterials.2013.11.037

24. Zanchetta E, Guidi E, Della Giustina G, et al. Injection molded polymeric micropatterns for bone regeneration study. *ACS Appl Mater Interfaces*. 2015;7(13):7273–7281. doi:10.1021/acsami.5b00481
25. Matschegewski C, Staehlke S, Loeffler R, et al. Cell architecture–cell function dependencies on titanium arrays with regular geometry. *Biomaterials*. 2010;31(22):5729–5740. doi:10.1016/j.biomaterials.2010.03.073
26. Yim EKF, Darling EM, Kulangara K, Guilak F, Leong KW. Nanotopography-induced changes in focal adhesions, cytoskeletal organization, and mechanical properties of human mesenchymal stem cells. *Biomaterials*. 2010;31(6):1299–1306. doi:10.1016/j.biomaterials.2009.10.037
27. Seo CH, Jeong H, Furukawa KS, Suzuki Y, Ushida T. The switching of focal adhesion maturation sites and actin filament activation for MSCs by topography of well-defined micropatterned surfaces. *Biomaterials*. 2013;34(7):1764–1771. doi:10.1016/j.biomaterials.2012.11.031
28. Hulshof FFB, Papenburg B, Vasilevich A, et al. Mining for osteogenic surface topographies: in silico design to in vivo osseo-integration. *Biomaterials*. 2017;137:49–60. doi:10.1016/j.biomaterials.2017.05.020
29. Li S, Chow T, Chu J. Engineering microdent structures of bone implant surfaces to enhance osteogenic activity in MSCs. *Biochem Biophys Rep*. 2017;9:100–105. doi:10.1016/j.bbrep.2016.11.016
30. Dolatshahi-Pirouz A, Pennisi CP, Skeldal S, et al. The influence of glancing angle deposited nano-rough platinum surfaces on the adsorption of fibrinogen and the proliferation of primary human fibroblasts. *Nanotechnology*. 2009;20(9):095101. doi:10.1088/0957-4484/20/9/095101
31. Lord MS, Foss M, Besenbacher F. Influence of nanoscale surface topography on protein adsorption and cellular response. *Nano Today*. 2010;5(1):66–78. doi:10.1016/j.nantod.2010.01.001
32. McBeath R, Pirone DM, Nelson CM, Bhadriraju K, Chen CS. Cell shape, cytoskeletal tension, and RhoA regulate stem cell lineage commitment. *Dev Cell*. 2004;6(4):483–495. doi:10.1016/S1534-5807(04)00075-9
33. Abagnale G, Sechi A, Steger M, et al. Surface topography guides morphology and spatial patterning of induced pluripotent stem cell colonies. *Stem Cell Rep*. 2017;9(2):654–666. doi:10.1016/j.stemcr.2017.06.016
34. Goriainov V, Cook RB, Murray JW, et al. Human skeletal stem cell response to multiscale topography induced by large area electron beam irradiation surface treatment. *Fron Bioeng Biotechnol*. 2018;6. doi:10.3389/fbioe.2018.00091
35. Biggs MJP, Richards RG, Gadegaard N, Wilkinson CDW, Oreffo ROC, Dalby MJ. The use of nanoscale topography to modulate the dynamics of adhesion formation in primary osteoblasts and ERK/MAPK signalling in STRO-1+ enriched skeletal stem cells. *Biomaterials*. 2009;30(28):5094–5103. doi:10.1016/j.biomaterials.2009.05.049
36. Wei D-X, Dao J-W, Chen G-Q. A micro-ark for cells: highly open porous polyhydroxyalkanoate microspheres as injectable scaffolds for tissue regeneration. *Adv Mater*. 2018;30:1802273.
37. Wu X, Wang S. Regulating MC3T3-E1 cells on deformable poly(ε-caprolactone) honeycomb films prepared using a surfactant-free breath figure method in a water-miscible solvent. *ACS Appl Mater Interfaces*. 2012;4(9):4966–4975. doi:10.1021/am301334s
38. Zhao C, Pan C, Sandstedt J, Fu Y, Lindahl A, Liu J. Combination of positive charges and honeycomb pores to promote MC3T3-E1 cell behaviour. *RSC Adv*. 2015;5(53):42276–42286. doi:10.1039/C5RA00756A
39. Zhang S, Ma B, Liu F, et al. Polylactic acid nanopillar array-driven osteogenic differentiation of human adipose-derived stem cells determined by pillar diameter. *Nano Lett*. 2018;18(4):2243–2253. doi:10.1021/acs.nanolett.7b04747